194
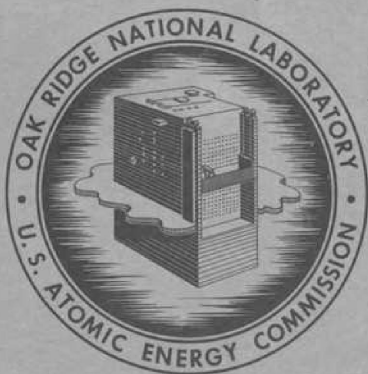
ORNL-2982
UC-4 – Chemistry-General

SELF-DIFFUSION OF CHROMIUM

IN NICKEL-BASE ALLOYS

R. B. Evans III
J. H. DeVan
G. M. Watson

OAK RIDGE NATIONAL LABORATORY
o   operated by
UNION CARBIDE CORPORATION
for the
U.S. ATOMIC ENERGY COMMISSION

Contract No. W-7405-eng-26

REACTOR CHEMISTRY DIVISION

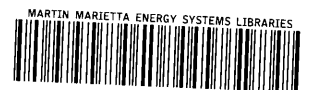# SELF-DIFFUSION OF CHROMIUM IN NICKEL-BASE ALLOYS

R. B. Evans III
J. H. DeVan
G. M. Watson

DATE ISSUED

JAN 2 0 1961

CONTENTS

SELF-DIFFUSION OF CHROMIUM IN NICKEL-BASE ALLOYS

R. B. Evans III   J. H. DeVan   G. M. Watson

ABSTRACT

The self-diffusion coefficients of Cr^{51} in Inconel and INOR-8, which are alloys suitable for use at high temperatures, were measured by contacting the alloys with fused salt mixtures containing radioactive chromous fluoride. These data are pertinent to the interpretation of corrosion behavior occurring in polythermal systems consisting of molten fluorides contained in nickel-base alloys. The diffusion coefficients were determined both by direct monitoring of the Cr^{51} intake by the alloys and in some cases by an analysis of the Cr^{51} concentration profile below the exposed surfaces of the metals. The experiments were designed to provide data over the temperature range 600 to 900°C, where relatively low diffusion coefficients (10^{-16} to 10^{-12} cm^2/sec) were obtained. At temperatures above 800°C the magnitudes of the diffusion coefficients obtained by both techniques were the same. At temperatures below 800°C the diffusion coefficients obtained from the concentration profiles were higher and had a lower temperature dependence than those obtained by direct monitoring of the intake of Cr^{51}. This was interpreted as implying that at the lower temperatures, diffusion occurs largely through selective paths, while at the high temperatures, homogeneous diffusion occurs. The observed diffusion coefficients can be expressed by the equation

$$D = D_0 e^{-E/RT} \quad .$$

The values of D_0 and E were found to vary, depending on the history of the specimen. For Inconel specimens annealed at 1150°C for periods of 2 hr or longer, the values of E ranged from 62 to 66 kcal/mole, and D_0 from 1.0 to 2.8 cm^2/sec. For the two alloys studied the observed diffusion coefficients were the same.

1

INTRODUCTION

Two primary requisites to be considered when selecting a suitable container material for molten fluoride mixtures are availability and compatibility with the salt. Based on these requisites alone, pure nickel is an obvious choice for many container applications. Additional requirements, such as air oxidation resistance and strength, are imposed when the applications involve polythermal reactor systems. Development work has clearly indicated that nickel-base alloys are suitable materials for reactor applications and constitute a workable compromise for the diverse requirements mentioned.[1]

Inconel and INOR-8 are two nickel-base alloys which have received a considerable degree of research attention during the last few years — particularly regarding fluoride corrosion resistance. It has been found that the corrosive attack incurred is selective toward chromium[2] and is initiated through chromium oxidation at the surface by traces of HF, NiF_2, FeF_2, and UF_4. The attack is relatively mild when the salt is properly purified. The residual attack may be due to UF_4 alone, the effects of which cannot be completely eliminated.

Past work also suggests that the over-all rate of the selective attack is primarily governed by the diffusion rates of chromium within the alloys.

The work covered in the present report deals with a series of experiments which should be directly related to the corrosion problem under discussion. The experiments had as their objectives the measurements of various "self-diffusion" coefficients of Cr^{51} in Inconel and INOR-8 at temperatures ranging from 600 to 900°C. It should be pointed out that the first experiments were performed elsewhere[3] through a subcontract arrangement.[4] These data have been utilized and considerably extended by the present investigators.

---

[1]W. D. Manly et al., "Construction Materials for Molten Salt Reactors," p 595 in Fluid Fuel Reactors (ed. by Lane, MacPherson, and Maslan), Addison-Wesley, Reading, Mass., 1958.

[2]Ibid., p 599.

[3]R. B. Price et al., A Tracer Study of the Transport of Chromium in Fluoride Fuel Systems, BMI-1194 (June 18, 1957).

[4]W. R. Grimes, ORNL, private communication, 1956.

This report is divided into three major sections: a presentation of experimental results involving over-all Cr^{51} diffusion rates, a presentation of the corresponding Cr^{51} concentration profiles, and an interpretation of the data in terms of a simple diffusion model.

EXPERIMENTAL APPROACH

Diffusion Coefficients

The diffusion coefficient is a flow-resistance parameter used in diffusion rate—time relationships. It is defined by the linear flow equation (Fick's first law)

$$\frac{1}{A} \frac{\partial M}{\partial t} = -D \frac{\partial C}{\partial x} \quad , \tag{1}$$

which, if steady-state conditions are established and D is assumed to be independent of concentration, may be written as

$$\frac{1}{A} \frac{\Delta M}{\Delta t} = D \frac{\Delta C}{L} \quad , \tag{2}$$

where

$\Delta M / \Delta t$ = constant rate of diffusion, g/sec,

A = area through which diffusion takes place, cm^2,

L = length, cm, of system in x direction (L is zero at the surface and increases with penetration of the metal wall),

ΔC = concentration change of diffusing material across L, $C_{x=0} - C_{x=L}$, g/cm^3,

D = diffusion coefficient, cm^2/sec.

The diffusion coefficient is a function of temperature, the diffusing material, and the material through which diffusion takes place. It does not depend on the macroscopic geometry of the flow system.

The steady-state equation (2) is useful for discussion and forms the basis for the determination of flow constants in analogous systems (flow of heat, flow of electricity, and fluid flow in porous media); however, its use in solid-state diffusion studies has been discouraged because of the extremely low values of $\Delta M / \Delta t$ and D involved. The only alternative is utilization of experiments and equations based on unsteady-state flow.

The basic linear flow equation for this case is

$$\frac{\partial C}{\partial t} = \frac{\partial}{\partial x} \left(D \frac{\partial C}{\partial x} \right) . \tag{3}$$

If self-diffusion measurements are to be made, for example, diffusion of radioactive silver into pure silver, and/or if the values of $\partial C/\partial x$ involved are not high, the diffusion coefficient can be treated as a constant. Under such conditions and at fixed temperature and pressure, Eq. (3) may be written as[5]

$$\frac{\partial C}{\partial t} = D \frac{\partial^2 C}{\partial x^2} . \tag{4}$$

Equation (4) is known as Fick's second diffusion law.

In the case of one-dimensional diffusion, applicable integrated forms of the above differential equations contain two independent variables, the time t and the coordinate x along which diffusion takes place. Consequently, development of equations relating the diffusion coefficient to measured variables requires knowledge of either the concentration profile along the path of diffusion at a given time or the variation of concentration with respect to time at a given coordinate. Both methods have been successfully employed for diffusion studies.

Tracer Techniques Applied to Diffusion Measurements

Several established techniques based on the use of radioactive iso-topes as tracers are available for measuring diffusion coefficients in metals. All the methods strive to establish experimental conditions such that the diffusion behavior can be conveniently described by using the fundamental diffusion equations discussed in the preceding section. The techniques differ widely, however, in the method of tracer placement and in the method of data analysis.

In the case of self-diffusion measurements, the method of tracer placement has generally involved the use of a diffusion couple, that is, a material containing a high percentage of radioactive atoms physically

---

[5]J. H. Wang, "Radioactivity Applied to Self-Diffusion Studies," in Radioactivity Applied to Chemistry (ed. by Wahl and Bonner), Wiley, New York, 1951.

4

joined to a material of similar chemical composition but of lesser radio-activity. The simplest mathematical solution describing the movement of diffusing atoms in such a couple results if the material of higher radio-activity is in the form of an infinitely thin layer (or plane source) and if the diffusing medium may be considered infinitely thick. The solution of Eq. (4) for this condition (assuming one-dimensional diffusion) is

$$C = \frac{Q_0}{(\pi Dt)^{1/2}} e^{-x^2/4Dt} \quad , \tag{5}$$

where C refers to tracer concentrations at depth x after time t, and the quantity Q_0 refers to an impulse (g/cm^2) of tracer supplied to the metal from the thin layer source. These boundary conditions are met experi-mentally only if the penetration distance is large compared with the orig-inal thickness of the tracer layer.

A convenient set of boundary conditions results from an experimental standpoint when both the tracer layer and the diffusing medium approach a thickness which can be regarded as infinite. The solution in this case becomes

$$\frac{C}{C_0} = \frac{1}{2} \left[1 + erf \frac{x}{2(Dt)^{1/2}} \right] . \tag{6}$$

In certain experiments placement of tracer atoms is effected through surface reactions. If by such a method the surface concentration of tracer atoms is brought instantaneously to and maintained at a constant level, a convenient solution of Eq. (4) results; namely,

$$C = C_0 \; erfc \; \frac{x}{2(Dt)^{1/2}} \quad . \tag{7}$$

Carburizing experiments in which labeled carbon activities are established at surfaces of metal specimens by exposing them to CO_2-CO or CH_4-H_2 gas mixtures are well-known examples[6] of this technique.

Three basically different approaches have been utilized to analyze the experimental results once the diffusion of tracer has been effected.

---

[6]L. S. Darken and R. W. Gurry, Physical Chemistry of Metals, p 450–51, McGraw-Hill, New York, 1953.

Most commonly the diffusion medium has been sectioned and the sections analyzed to obtain a concentration profile as a function of distance below the diffusion interface. In certain cases a surface counting technique has been employed;[7] in this technique the diffusion coefficient is calculated from the decrease in activity of the face of the specimen on which a thin layer of the radioactive isotope was originally deposited.

A more recently advanced method for determining the extent of tracer penetration is based on the use of autoradiography.[8] The experimental procedure is similar to that used in the sectioning technique except that a single section is cut on a plane which is slightly less than normal to the direction of diffusion. A film which is sensitive to the type of radiation emitted by the tracer is placed over this section. The exposed film results in a photograph of the distribution of the tracer. The photographic density can be correlated with tracer concentration to give a complete penetration curve.

Many of the previous experimental methods were developed to obtain magnitudes of the diffusion coefficients and, more basically, to gain an understanding of the mechanism of tracer invasion. In the present studies, however, it was desired foremost to determine the amount of chromium which would enter or leave the alloy as a function of surface concentration, time, and temperature, and the method selected was aimed at determining the rate at which the tracer entered the diffusion medium as well as the distribution of tracer within the medium. Accordingly, the experimental information determined includes all the processes which occur as the diffusion medium adjusts to the concentration driving force, not just the unit atomic process by which an atom moves to a neighboring lattice site.[9] The importance of this distinction becomes evident when it is realized that at least two distinct processes contribute to the diffusion of atoms in polycrystalline metals — diffusion occurring along grain boundaries

---
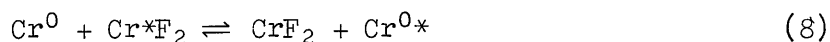
[7]G. Hevesy and W. Seith, Z. Physik 57, 869 (1929).

[8]S. T. Kishkin and S. Z. Bokstein, "Distribution and Diffusion of Components in Metal Alloys Studied by the Autoradiographic Method," Peaceful Uses of Atomic Energy, p 87, A/Conf 8/15, United Nations, 1955.

[9]C. Zener, "Theory of Diffusion," p 289 in Imperfections in Nearly Perfect Crystals (ed. by W. Shockley), Wiley, New York, 1952.

and diffusion through the grain matrix. In these studies no efforts were made to separate directly the effects of these two processes, although certain indirect observations of their relative magnitudes were permitted.

Present Experimental Methods

In the experimental methods employed for the present studies, the placement of radiotracer (Cr^{51}) was accomplished by means of the exchange reaction

$$Cr^0 + Cr^*F_2 \rightleftharpoons CrF_2 + Cr^{0*} \tag{8}$$

for which $\Delta F^\circ = 0$, $K_a = 1$, and $K_w \cong 1$. The Cr^*F_2 was dissolved in a carrier salt composed of $NaF-ZrF_4$ (53-47 mole %). This approach was suggested by the relative inertness of CrF_2, NaF, and ZrF_4 with respect to the primary constituents of Inconel (Ni, Cr, and Fe) and INOR-8 (Ni, Cr, Fe, and Mo). The chemical reaction between the salts and the metals under investigation was inconsequential;[10] hence the only reaction resulting at the surface was the exchange reaction (8) noted above, which created ratios of activated to nonactivated chromium atoms at the surface of the material identical with the ratios of activated to nonactivated chromium ions in the salt.

MEASUREMENT OF OVER-ALL DIFFUSION COEFFICIENTS

Depletion Method

If consideration is given to an alloy—molten salt system in which the molten salt initially contains dissolved CrF_2 and Cr^*F_2 and the alloy contains Cr^0 and no Cr^{0*}, a random exchange will take place as shown by Eq. (8), although the net change of total chromium is zero. The combined action of the exchange reaction and the diffusional forces within the alloy will result in a gain of Cr^{0*} in the alloy and a loss of Cr^*F_2 from

---

[10]A. Glassner, <u>The Thermochemical Properties of the Oxides, Fluorides, and Chlorides to 2500°K</u>, ANL-5750.

the salt. If the fractional depletion of Cr*F$_2$ activity in the salt (corrected for time decay) is measured as a function of time, a diffusion coefficient for chromium in the metal may be calculated by means of the following relationship:

$$\frac{b_{t=0} - b_t}{b_{t=0}} = 1 - e^{a^2 t} \text{ erfc } at^{1/2} = 1 - e^{u^2} \text{ erfc } u \quad , \tag{9}$$

where

t = time, sec,

$b_{t=0}$ = counts/g-min (at time count is made) of a filtered salt sample taken at $t = 0$,

b_t = counts/g-min (at time count is made) of a filtered salt sample taken at t,

a = depletion parameter, sec$^{-1/2}$,

$\quad = \dfrac{A}{V} \dfrac{[Cr^0]}{[CrF_2]} \dfrac{\rho_m}{\rho_s} D^{1/2}$,

A/V = ratio of the salt-exposed area of alloy to the salt volume, cm^{-1},

$[Cr^0]/[CrF_2]$ = weight fraction ratio of chromium in alloy to chromous fluoride (as Cr^{++}) in the salt,

ρ_m/ρ_s = density ratio of metal to salt,

D = diffusion coefficient, cm^2/sec,

u = $at^{1/2}$.

Equation (9) is based on a simultaneous solution of Eq. (4) and the equation resulting from a balance of the instantaneous transfer rates of labeled chromium from the salt to the metal, or

$$\frac{\partial}{\partial t} (M_{Cr*F_2}) = \left\{ -DA \frac{\partial}{\partial x} [C_{Cr^0*} (0,t)] \right\} \quad . \tag{10}$$

The variable x is distance within the alloy measured in the direction of diffusion, in cm; C_{Cr^0*} is concentration of Cr^0*, in g/cm^3; and M_{Cr*F_2} is the amount of Cr^{51} as Cr*F$_2$ in the melt.

The boundary conditions applied to obtain this solution are: (1) the alloy is infinitely thick in the x direction, (2) the initial concentration of Cr^0* in the alloy is zero, and (3) the concentration of Cr^0* at the alloy surface at any $t > 0$ is governed by Eq. (10) and varies with

time according to the relationship

$$[C_{Cr^0*}]_{x=0} = \rho_m [Cr^0] \frac{[Cr*F_2]}{[CrF_2]} \quad , \tag{11}$$

which stems directly from Eq. (8). Large-scale plots of u vs fractional depletion were used to convert the experimental data to the corresponding diffusion coefficients.

Experimental data have been obtained for two series of experiments, designated isothermal and polythermal, which satisfy the boundary conditions for Eq. (9). In the isothermal experiments, u was varied by varying t; all other parameters were held constant by charging an identical amount of salt to capsules of identical geometry and imposing isothermal conditions during the exposure period. These experiments afforded a direct verification of the time-dependence relationship for the depletion-type experiments.[11]

Constant-Potential Method

Initial experimentation indicated that the $Cr*F_2$ content of the molten salts in alloy containers will remain constant if, prior to the experiment, the temperature of the system is raised to 900°C for a few hours and then lowered. Depletion of $Cr*F_2$ is essentially stopped at the lower temperature by this procedure. Specimens in the form of 1/4-in.-OD Inconel thermocouple wells subsequently immersed in the salts absorb labeled chromium under conditions of a constant surface potential; that is, the Cr^0* concentration at the specimen surface remains constant with time. The corresponding Cr^0* transfer equation[12] is

$$\Delta M_{Cr^0*} = 2AC_{Cr^0*} \left(\frac{Dt}{\pi} \right)^{1/2} \quad . \tag{12}$$

---

[11]A description of the experimental details and the time-dependence curves may be found in the Appendix.

[12]J. H. Wang, "Radioactivity Applied to Self-Diffusion Studies," in Radioactivity Applied to Chemistry (ed. by Wahl and Bonner), Wiley, New York, 1951.

The variable C denotes concentration as g/cm^3. Rearranging Eq. (12),

$$D = \left(\frac{1}{16\pi t}\right)\left(\frac{y}{z}\frac{[CrF_2]}{[Cr^0]}\frac{1}{rh\rho_m}\right)^2 \quad , \tag{13}$$

where

    h = height of the immersed specimen,

    r = radius of the immersed specimen,

    y = total counts of the entire specimen (without alteration) per
        minute at t,

    z = counts of the salt per gram-minute at t.

The variable y is a measure of the total amount of tracer gained by the specimen; z is an indirect measure of the tracer concentration which is maintained on the specimen surface during immersion.

Four series of experiments were performed by means of the constant-potential method. Three series involved Inconel specimens which had been subjected to three types of pretreatment conditions; the fourth series involved INOR-8 specimens. The development and utilization of this method was partially stimulated by the need for tracer-containing alloy specimens for subsequent electropolishing experiments. Specimens from a constant-potential experiment were desirable in this respect as they were related to a convenient set of solutions of the diffusion equations. Further information regarding experimental details is presented in the Appendix.

<div align="center">Results</div>

Over-all coefficients, as a function of temperature and grain size, were obtained from six series of experiments. The experiments could be conveniently grouped according to experimental method, alloy pretreatment, and type of alloy. For brevity of presentation, an outline of the experiments is shown in Table 1.

Experimental points for groups I–IV and reported[13] high-temperature values for a similar alloy are plotted in Fig. 1. The experimental points for groups V and VI are not shown, since the general appearance, scatter, and slope of a plot of these points are very similar to those of Fig. 1.

---

[13]P. Gruzin and G. Federov, Doklady Akad. Nauk S.S.S.R. 105, 264 (1955).

Table 1. Summary of Experiments to Determine Over-All Diffusion Coefficients

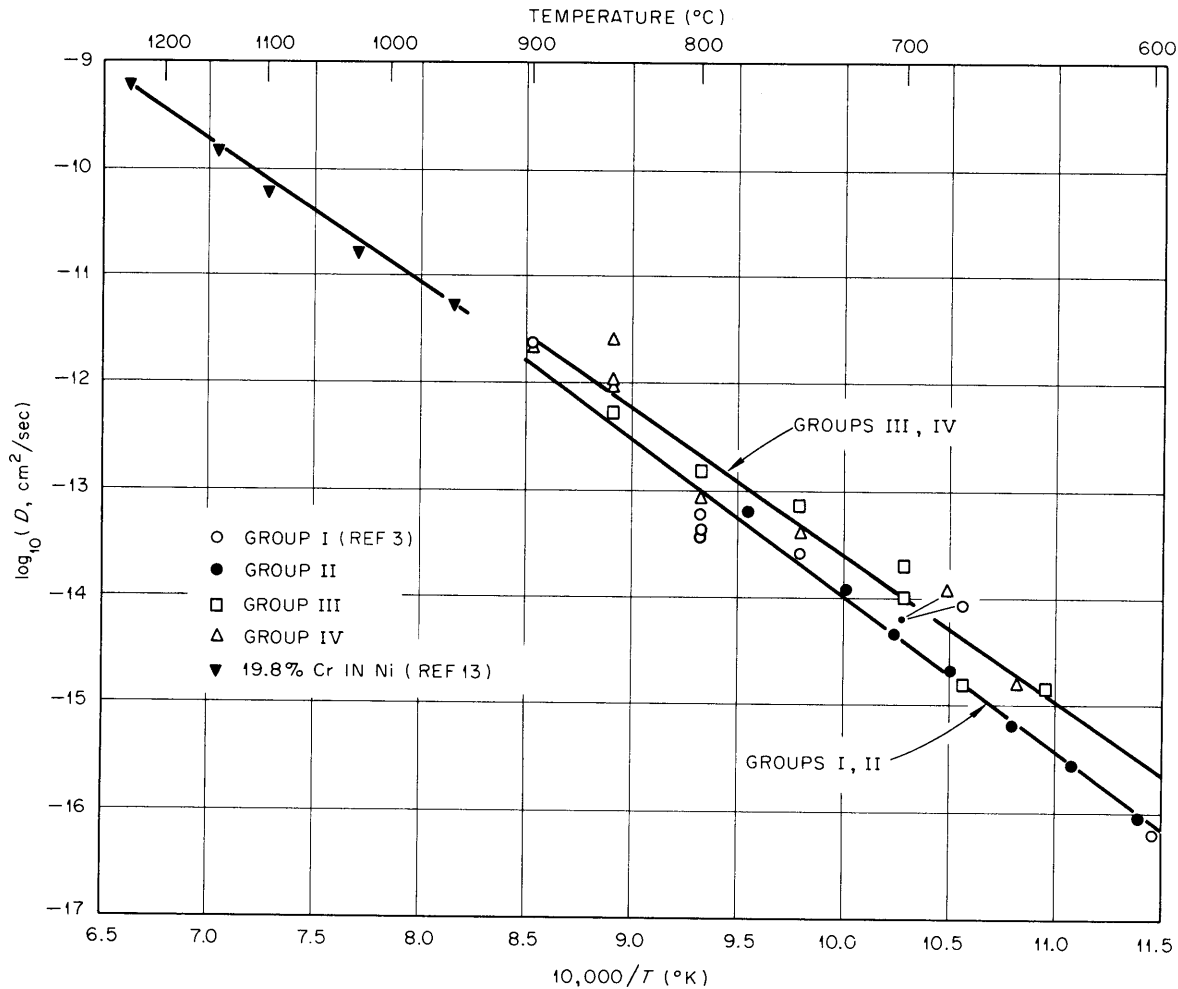| Experiment Group Number	Type of Experiment	Chromium Content of Alloy (wt %)	Solvent Composition (mole %)	Alloy Material and Dimensions	Alloy Pretreatment or Annealing Conditions	Remarks
I	Isothermal capsule (depletion)	16.0	$NaF-ZrF_4$ (50-50)	Inconel: sides, 3/8-in. tubing; bottom, plate	Welding temperature, then normalized under H_2 for 4 hr at 900°C	Previously uncorrelated data obtained from ref 3 at 3 temperatures
II	Polythermal capsule (depletion)	14.4	$NaF-ZrF_4$ (53-47)	Inconel: capsules machined from bar stock 3/8-in. OD, 5/16-in. ID, 25/64-in. inside length	Annealed under H_2 for 8 hr at 1150°C	Experiment performed to verify and augment group I results
III	Constant potential	15.2	$NaF-ZrF_4$ (53-47)	Inconel: 1/4-in. tubing, 0.035-in. wall	Annealed under H_2 for 2 to 4 hr at 1150°C	Several groups of isothermal experiments performed to verify Eq. (12) and to evaluate the experimental method
IV	Constant potential	15.1	$NaF-ZrF_4$ (53-47)	Inconel: 1/4-in. tubing, 0.035-in. wall	Annealed under He for 2 to 4 hr at 1150°C	Single 1-day exposure time; experiments performed to show effects of H_2 vs He annealing
V	Constant potential	14.8	$NaF-ZrF_4$ (53-47)	Inconel: 1/4-in. tubing, 0.035-in. wall	Annealed under H_2 for 8 to 12 hr at 800°C	Single 2-week exposure-time experiments performed to show effects of lower annealing temperatures and to provide specimens for electropolishing experiments
VI	Constant potential	7.03	$NaF-ZrF_4$ (53-47)	INOR-8: 1/4-in. tubing, 0.028-in. wall	Annealed under H_2 for 8 to 12 hr at 800°C	Single 2-week exposure-time experiments performed to obtain preliminary INOR-8 over-all coefficients comparable to Inconel coefficients

Fig. 1. Experimental Results for 1150°C Annealed Inconel. Over-all coefficients.

It should be mentioned that an isothermally determined over-all coefficient depends on the measurement, control, or knowledge of ten variables. Seven of these variables are squared in the final equation; also, the coefficient changes approximately 4% per degree centigrade at 700°. The maximum error in any single coefficient could be ±0.4 of a cycle on Figs. 1 and 2. This estimate excludes the effects of grain size variations.

The effect of temperature on the observed diffusion coefficients can be expressed by the equation

$$D = D_0 e^{-E/RT} \quad .$$

For the two solid lines labeled "groups I, II" and "groups III, IV," the values of E are 66 and 62 kcal/mole, and the values of D_0 are 2.8 and 1.0 cm^2/sec respectively.

In view of the over-all precision involved, the most realistic summary of the results might consist of a comparison of the average curves for all available data. Such a comparison is presented in Fig. 2.

Discussion and Conclusions

A comparison of results obtained with an unannealed Inconel specimen (point A, Fig. 2) and those obtained with three annealed specimens (point B, Fig. 2) presents a pointed illustration of effects associated with grain
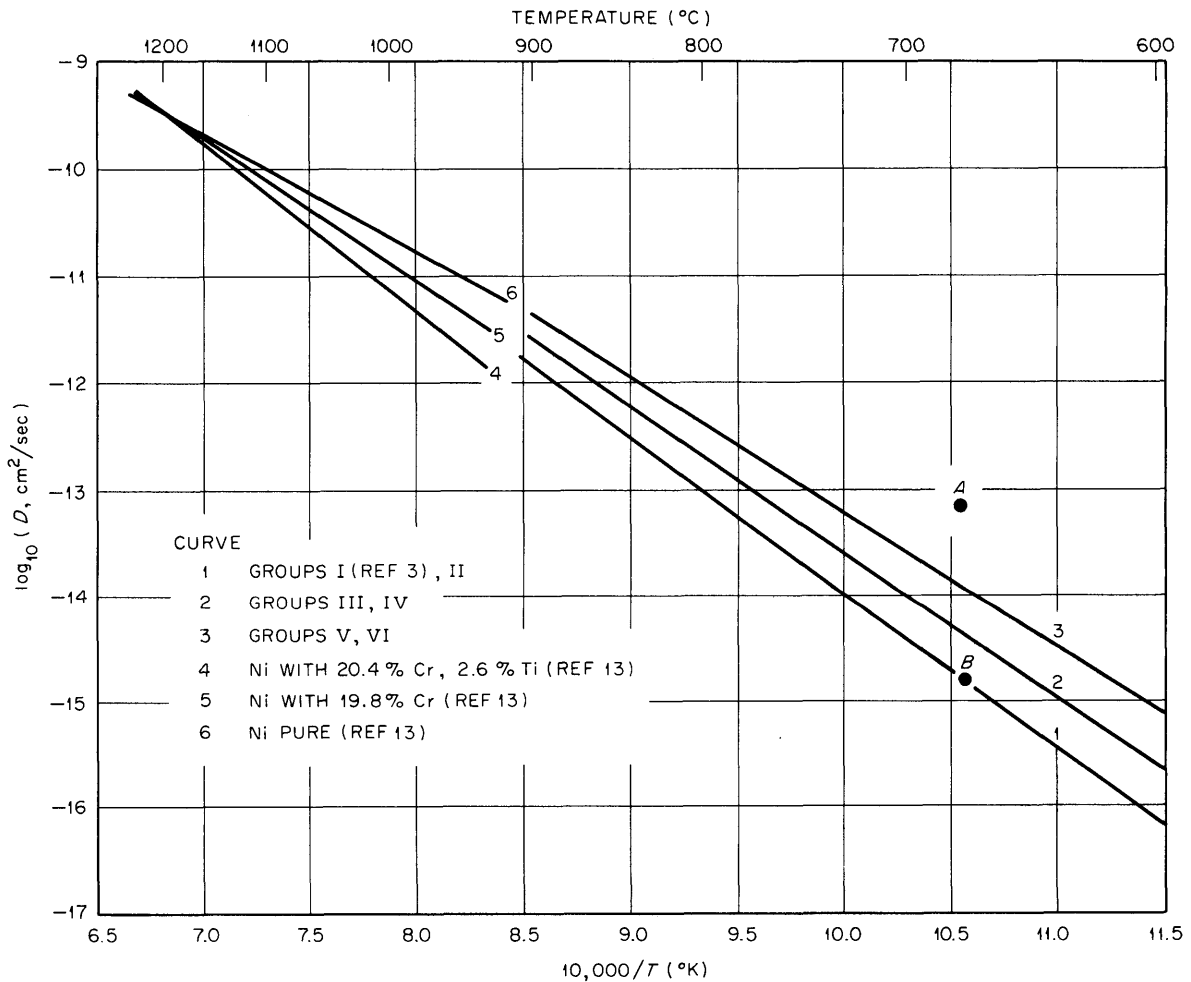
Fig. 2. Chromium-51 Diffusion Coefficients in Nickel-Base Alloys. Over-all values.

13

size. Photomicrographs showing the grain size of these specimens may be found in Fig. 3 (ref 14). Both the unannealed and the annealed specimens were exposed to the same pot-salt system at the same temperature. The same trend was shown by all the experimental results, in that increases in the time and temperature of pretreatment increased the grain size, which, in turn, led to a decrease in the over-all coefficient. It was concluded that grain size effects had a marked influence on the over-all diffusion coefficient.

The above conclusion formed the basis for another interpretation; that is, specimens with the highest number of grains also contained the highest number of "grain boundaries"; accordingly, one might suspect that a certain fraction of the diffusion took place along grain boundaries at temperatures around 700°C.

Thus there would be reason to think in terms of two coefficients, for example, volume and grain boundary. A treatment of a similar case by Fisher[15] and by Whipple[16] revealed that the time dependence of the penetration relationships would be altered when both mechanisms are combined. Such was not the case in this investigation. The data appeared to follow the equations presented. These equations were based on a single phenomenological coefficient which could be used to represent a homogeneous diffusion process taking place in an isotropic medium.

An encouraging feature of the results shown in Fig. 2 is the relatively good agreement between the high- and low-temperature data. A "break" in the over-all coefficient curves indicating a change in mechanism was not found for the Inconel specimens. The breaks noted in previous investigations (generally obtained from concentration profiles) result in relatively flat curves at low temperature regions.

Coefficients presented in Fig. 2 represent alloys with chromium contents ranging from 0 to 20.4 wt %. In view of the precision of the measurements and grain size effects, it was concluded that the over-all coefficients above 700°C did not depend on the chromium concentration in the INOR-8 and the Inconel. The amount of diffusion did depend on the concentration in a manner predicted by Eqs. (9) and (12).

---

[14]Additional photomicrographs are included in the Appendix.

[15]J. S. Fisher, J. Appl. Phys. _22_, 74 (1951).
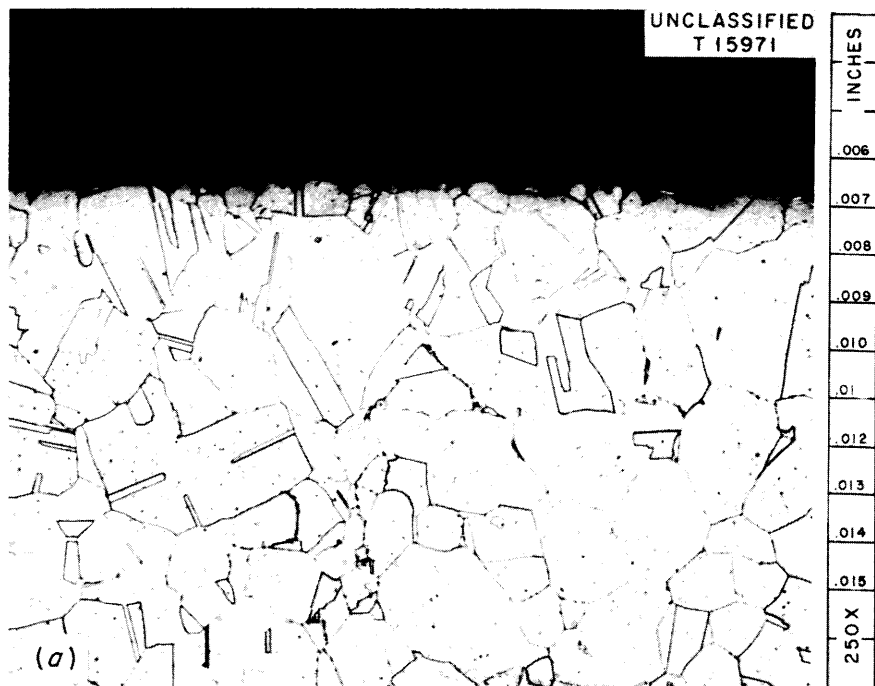
[16]R. T. P. Whipple, Phil. Mag. _45_, 1225 (1954).

Fig. 3. Photomicrographs of Annealed and Unannealed Inconel Specimens. (a) Specimen unannealed (point A, Fig. 2); $D = 78 \times 10^{-15}$ cm^2/sec. (b) Specimen annealed at 1150°C for 4 hr; $D = 1.7 \times 10^{-15}$ cm^2/sec. $T_{salt} = 675$°C for both experiments.

CHROMIUM-51 DIFFUSION COEFFICIENTS FROM
ELECTROPOLISHING EXPERIMENTS

Introduction

Practically all the solid-state diffusion data reported in the literature are based on the experimental determination of tracer concentration profiles as a function of penetration distance. The experiments differ as to the boundary conditions, tracer placement techniques, and sectioning procedures employed. However, determination of the tracer profile is the basic objective common to all experiments of this type. The profile data are then converted to diffusion coefficients through a knowledge of the proper concentration equations.

It was felt that a series of experiments of this type would constitute an interesting complement to the Inconel experiments discussed in the preceding section of this report. Two types of coefficients for a given specimen would be available. One would be based on the measurement of the over-all amount of tracer which diffused into the specimen under a known surface potential; the second would be based on the tracer concentration profile within the specimen.

Description of Method

Three major considerations governed the choice of a method for sectioning the tracer-containing specimens. First, very shallow tracer penetrations (very steep tracer concentration vs distance curves) would be involved; second, the operation should be fast and should not require particular skills; third, the specimens would be cylindrical in shape since they would originate from capsules, pots, or loops. It appeared that an electropolishing technique would satisfy all these requirements.

Based on the first two requirements mentioned, an integral method[17] was employed to correlate the data. This avoided the necessity of taking a large number of minute "cuts" and then having to calculate a large number of "average" concentrations. The experiments were conducted in the

---

[17]S. D. Gertsricken and I. Y. Dekhtyar, Proc. Intern. Conf. Peaceful Uses Atomic Energy, Geneva, 1955 15, 99 (1955).

following manner. After salt exposure, the specimens were counted, polished, re-counted, polished again, etc., until less than 10% of the original count was present. The percentages of total counts remaining after each polishing were plotted as a function of the cumulative penetration distances. The experimental plot was compared with a generalized plot of an equation applicable to the experimental procedure (constant potential, semi-infinite system, initial tracer concentration zero, etc.). The equation is

$$y(x) = 100(\pi)^{1/2} \int_X^\infty erfc\ w\ dw \quad , \tag{14}$$

where $y(x)$ is percentage of original activity remaining, and $w = x/2(Dt)^{1/2}$.

Values of Eq. (14) are available in the linterature.[18] A detailed description of the apparatus and procedures used to perform the electropolishing operation may be found elsewhere.[19]

Results

Present Investigation

Electropolishing experiments were performed on duplicate specimens obtained from 13 separate experiments mentioned in the preceding section (see group V). Of all the constant-potential specimens processed, this series contained the largest amount of tracer at the deepest penetrations. The final results are presented in Fig. 4 (open circles) immediately above the average curve, which represents the over-all coefficient obtained with the same specimens. It was interesting to note that the deviations exhibited by these data were faithfully reproduced by the over-all values on the lower curve.

Battelle Data

Electropolishing data submitted by Price[20] are shown on Fig. 5. In addition to the 800°C data shown, a meager amount of data was obtained

---

[18]H. S. Carslaw and J. C. Jaeger, _Conduction of Heat in Solids_, p 373, University Press, Oxford, 1950.

[19]J. H. DeVan, _An Evaluation of Electro-Machining for the Analysis of Metal Surfaces_, ORNL CF-59-6-109 (June 25, 1959).

[20]R. B. Price et al., _A Tracer Study of the Transport of Chromium in Fluoride Fuel Systems_, BMI-1194 (June 18, 1957).
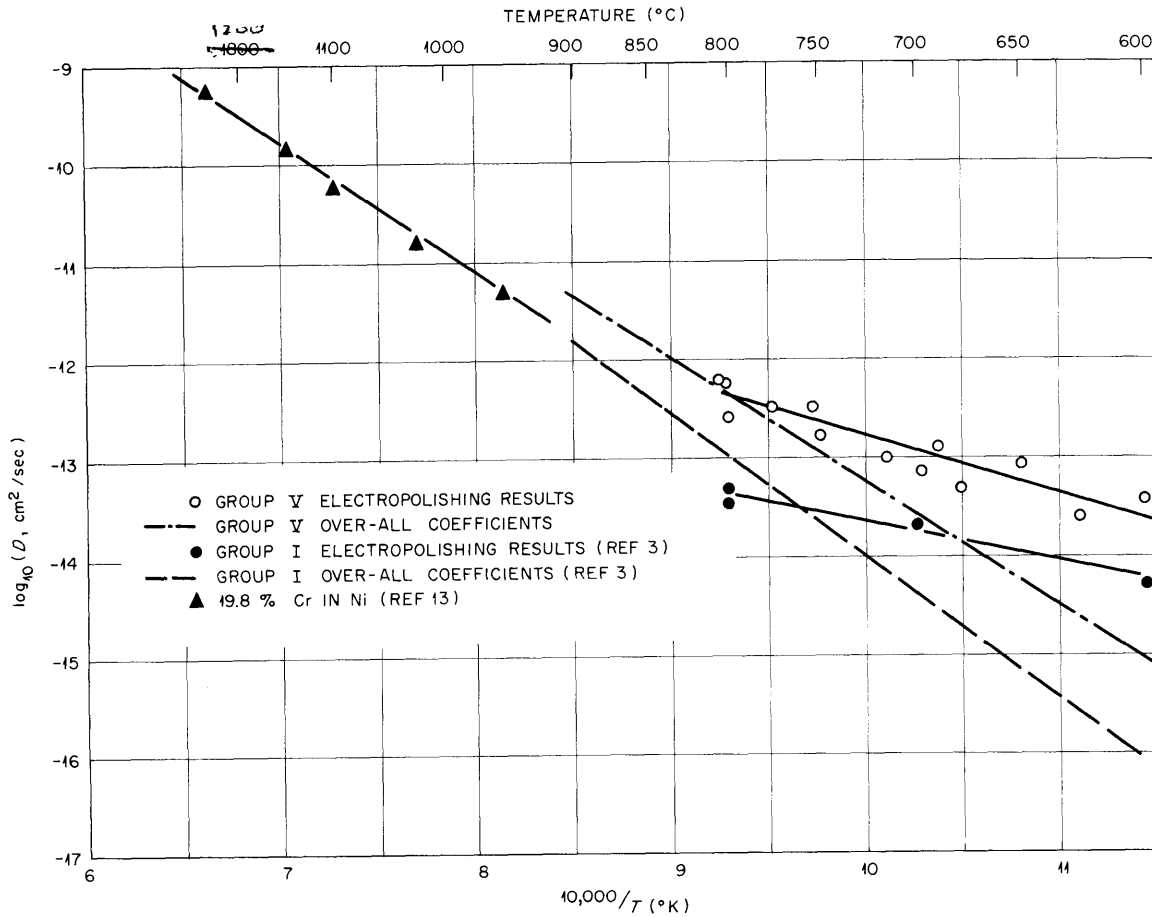
Fig. 4. Chromium Diffusion Coefficients for Inconel Based on Electropolishing Data.

for 700 and 600°C. The capsules used in the over-all depletion experiments served as the electropolishing specimens which led to these results. The rigorous profile equation for a depletion experiment is

$$C(x,t) = C_0 \ \text{erfc} \ \left[at^{1/2} + \frac{x}{2(Dt)^{1/2}} \right] \ \exp\left(\frac{ax}{D^{1/2}} + a^2 t \right) \ . \quad (15)$$

Since the required relationship would involve integration of Eq. (15) with respect to x, a decision was made to approximate the rigorous solution by means of Eq. (14). Past work had shown that analogous approximations with respect to the over-all transfer equations were acceptable. As it turned out, the approximate equation accurately described a major portion of the experimental profiles (see Fig. 5). Coefficients based
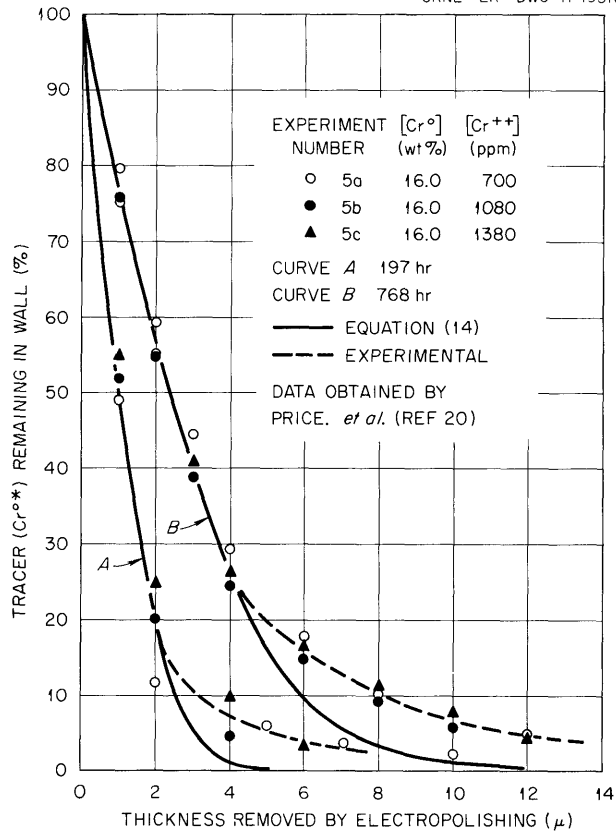
18

Fig. 5. Concentration Profiles in 800°C Depletion Capsules.

on the 800°C data[20] are shown in Table 2. All the available Battelle data are presented in Fig. 5.

Discussion

The 800°C data of Table 2 are of considerable importance, since the results of two independent series of experiments at this temperature established the equality of coefficients obtained from electropolishing experiments and over-all measurements. It is presently thought that equality of coefficients is a necessary condition for a homogeneous diffusion process.

The values given in Table 2 represent the results of three depletion experiments and six electropolishing experiments. The two profile coefficients shown were obtained from the average of three similar experiments. The number of over-all coefficients available corresponded to the number of capsule experiments (involving several capsules exposed for various

Table 2. Comparison of Diffusion Coefficients for Cr^{0*}
in Inconel at 800°C

By Cr^{0*} Concentration Profiles[a] (See Fig. 4)		By $[Cr^{++*}]$ Depletion[b]	
Salt Exposure Time (hr)	D (cm^2/sec)	$[Cr^{++}]$ (ppm)	D (cm^2/sec)
	$\times 10^{-14}$		$\times 10^{-14}$
197	3.47	700	4.25
768	4.75	1080	6.22
		1380	4.21

[a]Averages of curves for 700, 1080, and 1380 ppm Cr^{++} (see Fig. 5).

[b]Averages of several determinations with different exposure times at specific $[Cr^{++}]$ (see Fig. A.3).

times) that were performed, that is, three. It is important to note that the initial $[Cr^*F_2]/[CrF_2]$ ratio and the A/V ratio were identical for all experiments in the 800°C series. Thus, profiles for capsules with identical salt exposure times should be the same if the over-all diffusion equations previously presented and the assumed constant-potential boundary conditions were correct. It appears that these propositions are verified by the proximity of experimental points to the curves on Fig. 5.

As indicated by the curves of Fig. 4, the long anticipated "breaks" in the log D vs 1/T plots were finally acquired through the profile experiments. A discussion of the difference between these profile curves and curves for the companion over-all experiments will be given separately in the next section of this report.

ANALYSIS OF DIFFUSION DATA

It is observed from Fig. 4 of the preceding section that, at temperatures less than 800°C, the "diffusion coefficients" obtained from tracer concentration profiles are higher than those which were based on the total amount of tracer transferred. In order to correlate both kinds of coefficients, it is useful to visualize a diffusion specimen, wherein

the entire diffusion process occurs in intergranular channels. If it is assumed that all the channels can be grouped together to give a certain fraction, f, of the bulk volume, V_b, then fV_b will be the "active" volume and $(1 - f)V_b$ will be the "inactive" or dead volume. The next step concerns the selection of a reference coefficient for the active volume.

One of two suitable reference coefficients might be chosen; they are: a bulk coefficient, D_b, resulting from steady-state diffusion experiments, and a grain boundary (or channel) coefficient, D_g, which is based on studies of single grain boundaries. To precisely illustrate the meaning of the two hypothetical coefficients, a numerical example incorporating both coefficients was prepared. The example involved steady-state diffusion of tracer M through a metallic membrane 1.5 μ thick, 1.025 cm^2 in cross-sectional area, 10 wt % M, and 0.1 volume fraction, f. The membrane contained four active channels with dimensions given in Table 3. Both coefficients are based on the same driving force, ΔC, as indicated by

$$\frac{\Delta M}{\Delta t} = D_g \left(\Sigma \frac{A}{L_g} \right) \Delta C_M \quad , \tag{16}$$

since

$$C_b = C_g \text{ at } x = 0 \text{ and } L \quad ,$$

and

$$C_b = fC_g, \; 0 < x < L \quad .$$

Table 3. Channel Parameters for Hypothetical Membrane

Channel Number	Length (μ)	Area (cm^2)	Volume (cm^3)	A/L (cm)
		$\times 10^{-2}$	$\times 10^{-6}$	
1	3.0	2.50	7.500	83.3
2	1.5	1.25	1.875	83.3
3	2.0	1.75	3.500	87.5
4	5.0	0.50	2.500	10.0
		NA_g = 6.00	NV_g = 15.375	$\Sigma(A/L)$ = 264.1

21

Subscript b refers to bulk values; subscript g refers to channel or grain boundary values. For the example, D_g and ΔC_M were assumed to be 2×10^{-10} cm^2/sec and $(10 \text{ g/cm}^3) (0.1) (1.0 - 0.2) (10^{-8})$ respectively. The weight fractions were 1.0×10^{-8} and 2.0×10^{-9} at the surfaces. The corresponding rate was 4.23×10^{-16} g/sec. The bulk coefficient was obtained through the relationship

$$D_b = D_g \left(\frac{L_b}{A_b}\right) \sum_1^N \left(\frac{A_g}{L_g}\right)_i \quad , \tag{17}$$

with the assumed D_g and membrane dimensions given in Table 3; the D_b value was 7.73×10^{-12} cm^2/sec, which is considerably lower than the D_g value.

In many instances it will be very difficult to obtain individual A/L values, which are necessary for the utilization of a true D_g. However, a model D_g or $(D_g)_{model}$ may be estimated by visualizing a parallel series of channels with equal lengths and areas. By using the example values for NA_g, A_b, f, and D_b and the equations

$$NA_g L_g = f A_b L_b \quad , \tag{18a}$$

$$ND_g \frac{A_g}{L_g} = \frac{D_b A_b}{L_b} \quad , \tag{18b}$$

which describe the model, a $(D_g)_{model}$ value of 2.255×10^{-10} cm^2/sec was obtained. This value is in very good agreement with the original value of 2.0×10^{-10} cm^2/sec.

The foregoing example demonstrates that utilization of the model D_g would require information as to the average internal geometry of the diffusion media. This is not required for D_b. Nevertheless, reasonable estimates of channel behavior (D_g) can be made through D_b, since large errors are not introduced by the model when reasonable channel-size distributions are involved. Accordingly, D_b was selected as the reference coefficient for present interpretations.

The active-volume concept implies that tracer does not accumulate in the dead volume. Thus, Fick's law, from which equations describing

the experiments are developed, must be modified such that

$$D_b \frac{\partial^2 C}{\partial x^2} = f \frac{\partial C}{\partial t} \quad .$$ (19)

Applicable boundary conditions are

$$\lim_{x \to \infty} C(x,t) = 0 \quad ,$$ (20a)

$$C(x,0) = 0 \quad ,$$ (20b)

$$C(0,t) = C_0 \quad ,$$ (20c)

which lead to a solution

$$C(x,t) = f C_0 \text{ erfc } \frac{x}{2(D_b t/f)^{1/2}} \quad .$$ (21)

The corresponding equations for over-all tracer transfer, ΔM, and fraction of tracer remaining after electropolishing, y, are

$$\Delta M = 2 A C_0 \left(\frac{D_b f t}{\pi} \right)^{1/2} \quad ,$$ (22)

$$y(x) = 100(\pi)^{1/2} \int_x^\infty \text{ erfc } w \, dw \quad ,$$ (23)

$$w = \frac{x}{2(D_b t/f)^{1/2}} \quad .$$ (24)

These equations are compatible with the data in that the basic form of the time-dependence curves corresponding to Eq. (22) and the shape of the polishing profiles of Eq. (23) are not altered by the introduction of f. Furthermore, "low" over-all coefficients are predicted by $D_b f$ and "high" polishing coefficients by D_b/f. From the data and the present interpretation, values of $D_b f$ and D_b/f were measured during the experiments. Thus,

$$D_b = (D_{\text{over-all}} \cdot D_{\text{polish}})^{1/2} \quad ,$$ (25)

$$f = \left(\frac{D_{\text{over-all}}}{D_{\text{polish}}} \right)^{1/2} \quad .$$ (26)

The term "grain boundary diffusion," as it is generally used, refers to the portion of the electropolishing curves which have been ignored in this investigation, that is, the residual 5 to 15% of the total tracer transferred which undergoes comparatively deep penetration.

This interpretation applies to 85 to 95% of the material normally classified as "volume" diffusion. We submit that this fraction of the transferred tracer follows selective diffusion paths given by fV_b. Further, the value of f is unity at approximately 800°C for chromium in Inconel and decreases markedly with temperature reductions below 800°C.

CONCLUSIONS

As a result of the present investigation the following conclusions are apparent:

1. Self-diffusion coefficients of chromium in Inconel in the temperature range 600 to 900°C were conveniently determined (a) by monitoring the total intake of Cr^{51} by the alloys exposed to salt solutions containing $Cr*F_2$ and (b) by measuring the tracer concentration profiles through successive electropolishing of the specimens.

2. The experimental precision of the measurements was ±0.4 cycle, exclusive of effects related to the history of the specimen.

3. The self-diffusion coefficients of chromium in Inconel were found to be strongly dependent on annealing conditions at low temperatures. Conditions leading to large grains led to low diffusion coefficients and vice versa within this temperature range.

4. At temperatures above 800°C the magnitudes of the self-diffusion coefficients of chromium obtained by the different techniques were the same. At lower temperatures the diffusion coefficients calculated from the concentration profiles were higher and had a lower temperature dependence than those obtained by direct monitoring of the intake of Cr^{51}.

5. Deviations exhibited by the diffusion coefficients obtained by direct monitoring of the intake of Cr^{51} were faithfully reproduced by the corresponding values obtained from the concentration profiles, showing that specimen variations were not completely overcome by annealing pretreatment.

6. From the determination of the Cr^{51} concentration profiles, it was apparent that about 15% of the tracer penetrated deeper than calculated, using a single diffusion coefficient. This effect is believed to be due to "grain boundary diffusion." The bulk of the tracer penetration (85%) could be calculated in terms of a single coefficient.

7. No change in the time dependence of the penetration relationships was found at any temperature investigated.

8. The change in the temperature dependence noted for the coefficients obtained from concentration profiles indicates a change in the diffusion mechanism at about 800°C from homogeneous volume diffusion at high temperatures to diffusion along selective paths at low temperatures.

NOMENCLATURE

a	depletion parameter, $\sec^{-1/2}$
A	cross-sectional area normal to diffusion, cm^2
b	count rate of depletion salt sample, counts/g-min
C	Cr^{0*} (tracer) concentration, g/cm^3
C_0	Cr^{0*} (tracer) concentration initially at alloy surface, g/cm^3
$[CrF_2]$	chromous fluoride concentration in salt, ppm or weight fraction
$[Cr^0]$	chromium concentration in alloy, wt % or weight fraction
D	self-diffusion coefficient for chromium in alloy, cm^2/sec
D_b	bulk self-diffusion coefficient, cm^2/sec
D_g	channel self-diffusion coefficient, cm^2/sec
D_0	frequency factor, cm^2/sec
E	activation energy, cal/mole
f	fraction of bulk volume engaged in diffusion process
h	height or length of alloy specimen, cm
K_a	thermodynamic equilibrium constant, dimensionless
K_w	equilibrium quotient in terms of weight fractions of the components, dimensionless
L	length along path of flow, cm
M	total amount of Cr^{0*} present in alloy, g
N	number of channels involved in diffusion
Q_0	amount of Cr^{0*} per unit area of surface, g/cm^2
r	radius of cylindrical alloy specimen, cm
R	gas constant, cal $mole^{-1}$ $(°K)^{-1}$
ρ_m	alloy density, g/cm^3
ρ_s	salt density, g/cm^3
t	diffusion time, sec
T	temperature, °K
u	dimensionless diffusion time, $at^{1/2}$
V	salt volume, cm^3
w	dimensionless diffusion variable, $x/2(Dt)^{1/2}$
x	diffusion coordinate along L, cm
y	count rate of alloy specimen, counts/min
z	count rate of constant-potential salt sample, counts/g-min

APPENDIX

Materials

Chromium Tracer

Chromium tracer was introduced to the alloy-salt systems as Cr^{51}-labeled chromous fluoride for all the experiments mentioned in this report. This material was prepared initially in small amounts by a method described in detail by Sturm.[1,2] Briefly, the procedure involved adding 1 to 2 cm^3 of dissolved $Cr^{51}Cl_3$ (as received from the ORNL isotope facilities) to a suitable amount of $CrCl_3$ (approx 10 to 20 g), fusing with NH_4HF_2, decomposing in a hydrogen atmosphere, and then reducing with hydrogen; the resulting CrF_2 was found to contain metallic chromium in variable amounts with additional materials whose identities were not established. To obtain a pure material, crystals from large batch preparations were carefully selected and analyzed by Sturm;[1,2] these crystals were ground to pass 100-mesh screens and then subjected to neutron irradiation for one to two weeks. The Cr^*F_2-CrF_2 mixtures thus obtained were used without further dilution (with unlabeled chromous fluoride) for the experiments. At concentrations of 1500 to 3000 ppm in the base salt, the dissolved labeled material resulted in initial base salt count rates of 5×10^5 to 1×10^6 counts/g-min.

Molten Fluoride Solvent

Continued use of NaF-ZrF_4 mixtures as the molten salt solvent or base salt for all experiments was dictated by several considerations. Of primary importance were the noncorrosive and relatively nonhygroscopic properties of the solidified salt, since it was necessary to manipulate and store the alloy specimens after salt exposure. Further, the zirconium-base salts scavenge oxygen which might be inadvertently introduced to the system via moisture or structural metal oxides; the resulting HF can be rapidly removed through stripping with hydrogen, which also represses the buildup of NiF_2 and FeF_2. Alloy surfaces exposed to these solvents were

---

[1]B. J. Sturm, MSR Quar. Prog. Rep. Oct. 31, 1958, ORNL-2626, p 107.
[2]B. J. Sturm, ORNL, private communication.

in excellent condition even after two-week exposure periods. The solvent
densities as functions of temperature are given by the equations[3]

$$\rho \ (g/cm^3) = 3.79 - 0.00093t \ (°C)$$

for NaF-ZrF$_4$ (50-50 mole %) and

$$\rho \ (g/cm^3) = 3.71 - 0.00089t \ (°C)$$

for NaF-ZrF$_4$ (53-47 mole %).

Alloys

Information regarding the chromium content, type of alloy, and pre-
test treatments of the alloy specimens studied may be found in the main
body of this report (see Table 1 and Fig. 3). In addition, averages of
several analyses of the alloys are presented as nominal values in Table
A.1. Photomicrographs of typical specimens of experimental groups III,
IV, V, and VI are shown in Figs. A.1 and A.2; corresponding annealing
conditions are repeated in the titles for the reader's convenience. In
the calculation of the results, the numerical values used for the alloy

---

[3]S. I. Cohen, W. D. Powers, and N. D. Greene, A Physical Property
Summary for ANP Fluoride Mixtures, ORNL-2150 (Aug. 23, 1956).

Table A.1. Nominal Composition of Alloys Used for Experiments

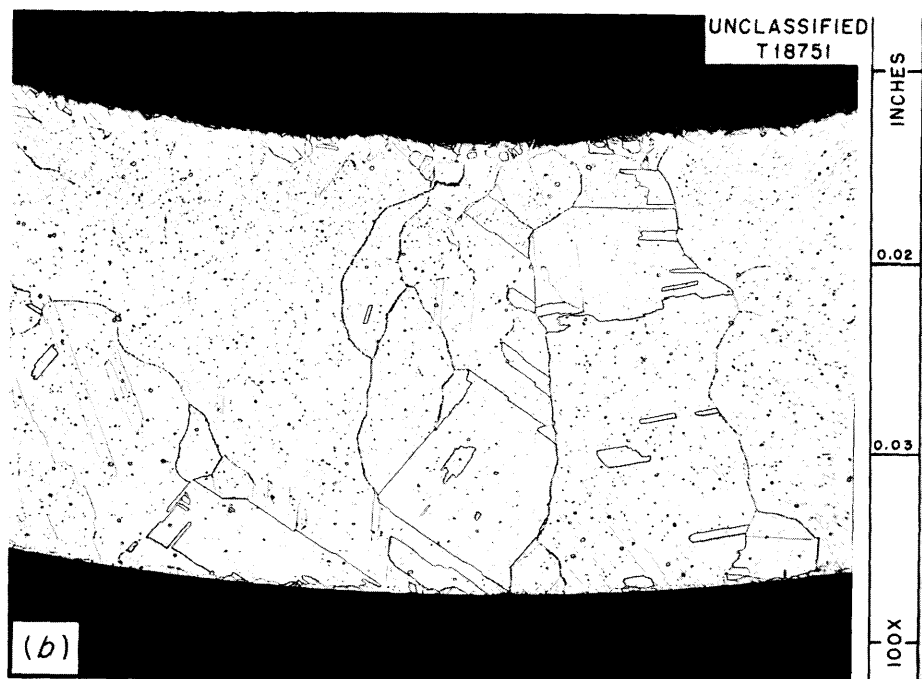|	Inconel	INOR-8
Cr	15.1%	7.0%
Fe	8.4%	5.1%
Ni	75.6%	71.0%
Mo	700 ppm	16.0%
Mn	3200 ppm	3700 ppm
Si	1800 ppm	3900 ppm
Ti	2800 ppm	Trace
Al	1500 ppm	200 ppm
B		Trace
C	800 ppm	700 ppm

Fig. A.1. Photomicrographs of Typical Group III and Group IV Speci-
mens. (a) Group III specimen H_6: Inconel annealed under hydrogen for 2
to 4 hr at 1150°C; (b) group IV specimen I-2: Inconel annealed under
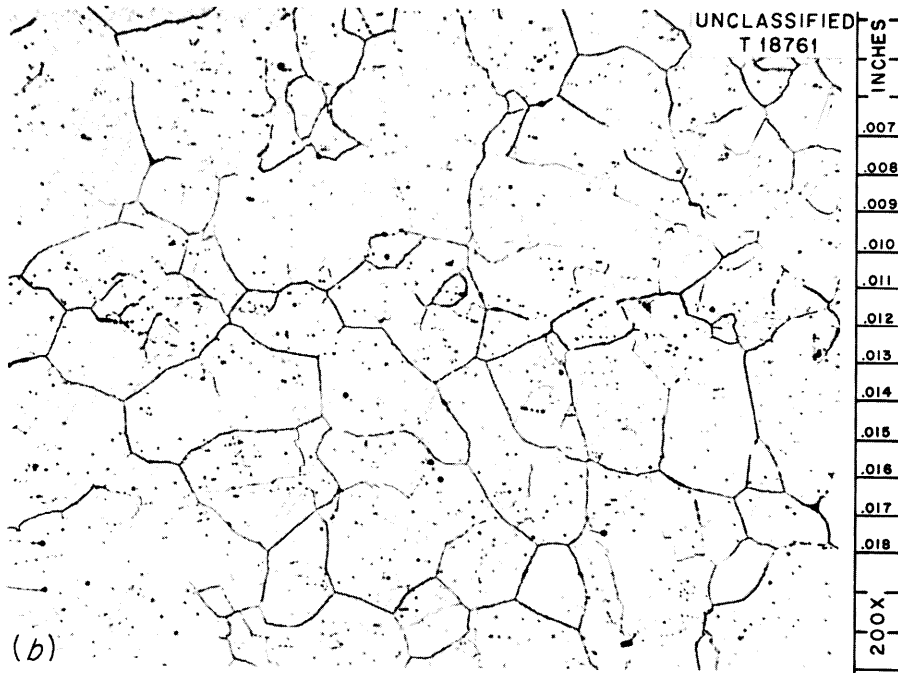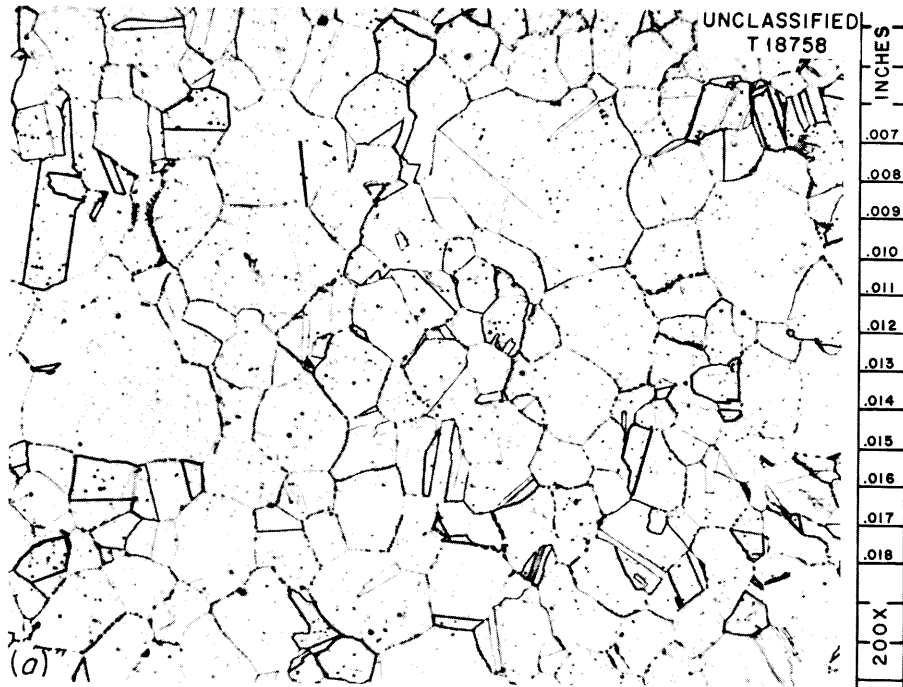helium for 8 to 12 hr at 1150°C.

Fig. A.2. Photomicrographs of Typical Group V and Group VI Speci-
mens. (a) Group V specimen J-13: Inconel annealed under hydrogen for
8 to 12 hr at 800°C; (b) group VI specimen K-5: INOR-8 annealed under
hydrogen for 8 to 12 hr at 800°C.

densities[4,5] at 20°C were 8.43 and 8.79 g/cm^3 for Inconel and INOR-8 respectively. Correspondingly, the coefficients for thermal expansion employed were 16.1×10^{-6} and 13.7×10^{-6} (°C)$^{-1}$.

Counting Techniques

A well-type scintillation counter was employed for all count-rate determinations which involved the gamma-emitting, 27.5-day-half-life Cr^{51}. Undesirable geometry and shielding effects which might introduce counting errors were minimized in the capsule (depletion) experiments, since the ratio of the count rates of equal amounts of salt in identical containers was employed.

Error considerations were somewhat more complex for the case of the constant-potential experiments; here, the measured coefficient depended on the count rate ratio of the Cr^{0*} embedded in a metal to the Cr*F$_2$ present in 1 g of salt. Although the same type of glass tubes was used to contain the metals and salts during counting, this was not sufficient to cancel all the shielding and geometry effects present. A series of metal specimens (1-in. lengths of 1/4-in. tubing) was counted with and without close-fitting nickel and Inconel slugs in the inside opening. No appreciable change in counts was obtained. It was concluded that little could be done to improve the accuracy of the measurement, such as increasing the inner diameter or dissolving the Cr^{0*} prior to counting.
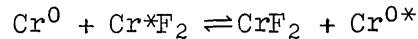
An experiment was then performed to determine the effect of specimen height, since the relative positions and heights of the salt samples and alloy specimens were not the same while undergoing count-rate determinations. Successive counts of an alloy specimen of uniform activity were obtained as the length was decreased. The same approach was applied with respect to the salt by addition of salt. Based on these data an appropriate correction was determined and applied to all constant-potential data. Additional doubts as to the effectiveness of this correction were dispelled through comparisons of the experimental coefficients for similarly annealed constant-potential data and those for the capsule data.

---

[4]Technical Bulletin T-7: Engineering Properties of Inconel and Inconel-X, International Nickel Co., Inc. (June 1953).
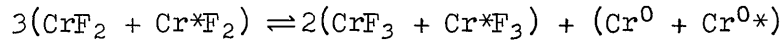
[5]A. Taboada, ORNL, private communication.

Wall Exchange Reaction

Use of the wall exchange reaction

$$Cr^0 + Cr^*F_2 \rightleftharpoons CrF_2 + Cr^{0*}$$

implies that no disproportionation such as

$$3(CrF_2 + Cr^*F_2) \rightleftharpoons 2(CrF_3 + Cr^*F_3) + (Cr^0 + Cr^{0*})$$

exists. The latter possibility caused concern during the early stages of this work and thus merits some discussion. Prior to the reported polythermal capsule experiment, a dummy run using tracer and welded nickel capsules was performed ostensibly to check manual procedures and the temperature profile in the polythermal block, with loaded capsules to obtain proper heat capacity, conductivity, etc. At the conclusion of the run it was found that the tracer initially present in the salt had undergone slight depletion in capsules which had been at 700°C or higher. The possibility of the formation of insoluble chromium oxides was rejected, since ZrF_4 was present in large amounts. Thus the observed depletion could have been due to the disproportionation reaction; even though the calculated standard free energy change for this reaction does not give evidence of disproportionation, the fact remains that the initial Cr^0 content of the metal was zero. In any event, other observations during experiments with alloys present lead to the conclusion that disproportionation is completely repressed when chromium is initially present in the walls and ZrF_4 is present in the solvent. For example, good agreement was obtained between high-temperature over-all and polishing coefficients. Also, the chromium concentration in salts continually exposed to fresh alloy specimens and variable temperatures remained constant with time. This might not be true if solvents other than those utilized were employed.

Procedures for Capsule Experiments

Isothermal Experiments

A detailed description of the procedures utilized to perform the isothermal capsule (depletion) experiments is given by Price.[6] The salient points are presented here for the reader's convenience.

---

[6]R. B. Price et al., A Tracer Study of the Transport of Chromium in Fluoride Fuel Systems, BMI-1194 (June 18, 1957).

Equal amounts of a prepurified solvent containing identical concentrations of Cr^*F_2 and CrF_2 were charged to several Inconel capsules of the same dimensions. A portion of the solvent was retained for the "time-zero" standard. The charged capsules were then sealed by welding and placed in an isothermal furnace. At various time intervals a single capsule was removed until the entire series had been transferred. The capsules were opened, the salt was removed, and the percentage or fraction of the original counts which had been lost was determined. These data were presented in graphical form as percentage loss vs time at temperature. The present investigators carefully transposed these data to plots as shown in Fig. A.3; the curves represent Eq. (9) evaluated with the average coefficient for a given experiment.

It should be noted that the points follow the curves reasonably well. Thus Fig. A.3 demonstrates that the time-dependence characteristics predicted by Eq. (9) are followed. Also, the data of Fig. A.3 show that increases in the amount of unlabeled material present result in decreased rates of depletion as predicted by the definition of a and/or u [see Eq.
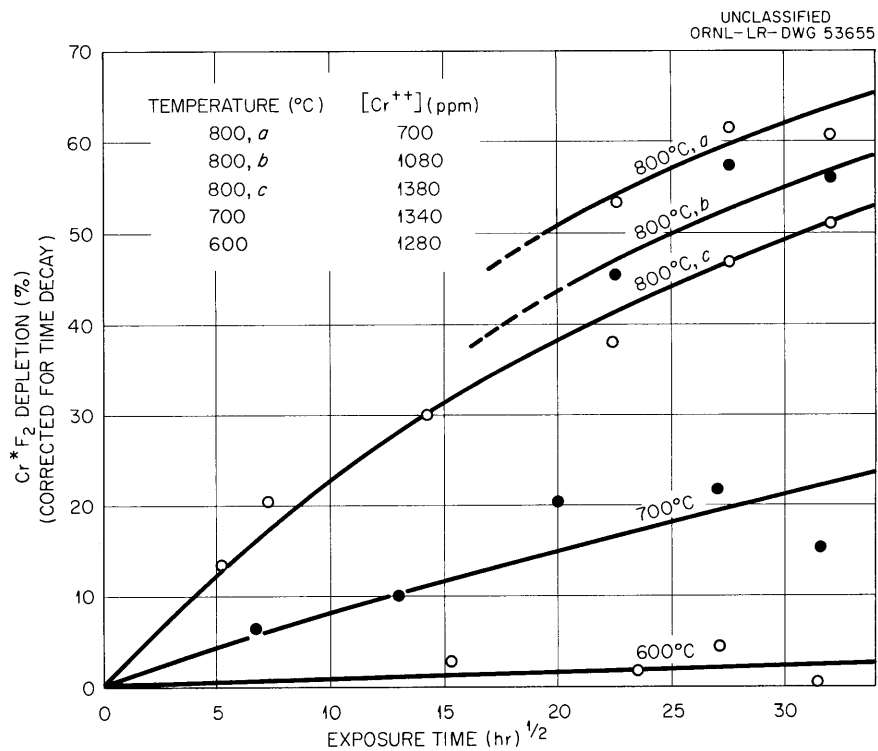
TEMPERATURE (°C)	$[Cr^{++}]$ (ppm)
800, a	700
800, b	1080
800, c	1380
700	1340
600	1280

Fig. A.3. Depletion of Cr^*F_2 from NaF-ZrF_4 (50-50 Mole %) Contained in Inconel.

33

(9)]. The average diffusion coefficients were obtained by comparing the experimental curves with a generalized plot of fractional depletion vs u (see curve A, Fig. A.4). This procedure was repeated until a satisfactory fit was obtained. The average values of the coefficients are presented in Fig. 1.
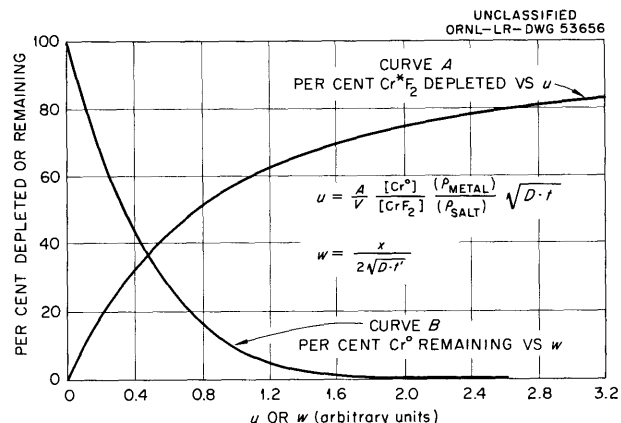

Fig. A.4. Theoretical Curves for Depletion and Electropolishing Experiments.

Polythermal Experiments

The polythermal depletion experiments were based on the use of a thermal gradient block similar to those described by Barton[7] for use in molten salt phase studies. With this device, over-all diffusion coefficients at several temperatures could be obtained from a single series of capsules.

Approximately 250 g of prepurified solvent was melted in an Inconel container, the labeled chromous fluoride was added (approximately 1 g), and the melt was then subjected to a stream of hydrogen at 700°C for 30 min. Portions of this mixture were then withdrawn by means of hydrogen-fired copper filter sticks. The filtered material was removed, ground to pass a 100-mesh screen, and transferred to pretared glass containers; these operations were carried out in an air-filled dry box. After initial counting and weighing, the salts and capsules were placed in a helium-filled dry box, wherein all caps were removed. The box was evacuated

---

[7]C. J. Barton et al., J. Am. Ceram. Soc. 41, 63 (1958).

overnight, refilled with helium, and the salt transferred to the capsules, which were then sealed by means of 3/8-in. Swagelok fittings. A hydrogen-fired nickel disk was placed on top of the capsules (prior to closure) to avoid contamination of the salt by removal of the oxidized fittings at the end of the experiment. All capsules were placed in the preheated furnace simultaneously by means of an Inconel tray. The temperature gradient was re-established within 30 min without overheating any of the capsules. At the end of several weeks, the tray was removed and all capsules were immediately quenched. The capsules were opened and the final counts and weighing were performed in the glass tubes used at the start of the experiment. Depletions were based on a portion of the starting material. The salts and alloys were then analyzed for total chromium content.[8]

Before the actual determination, a calibration run was made for determining the temperature gradient within the block as a function of capsule position for a given set of furnace conditions. Each capsule was charged with a different amount of salt containing the same labeled and unlabeled chromium fluoride concentration. All capsules were exposed to molten-salt temperatures over the same time interval. The amount charged was varied such that the factor $A_m \rho_m / M_s \rho_s$ would be constant, even though the temperatures of each capsule would be different. Thus the depletion equation could be used, with temperature acting as the independent variable.

The experimental points are plotted in Fig. A.5. The curve is based on a plot established on semilog paper. It can be shown that a semilog plot of depletion (as per cent) vs $1/T$ [$(°K)^{-1}$] will approximate a straight line at low values of depletion (low temperatures), deviating slightly at higher depletion values. This results from the exponential variation of D with respect to $1/T$ and affords a convenient method for correlating the experimental data.

Depletion values at the experimental temperatures were taken from the curve of Fig. A.5 and compared with the generalized plot of Fig. A.4. The data, thus smoothed, formed the basis for the group II coefficients presented in the main body of this report.

---

[8]This work was performed by W. F. Vaughan of the Analytical Chemistry Division.
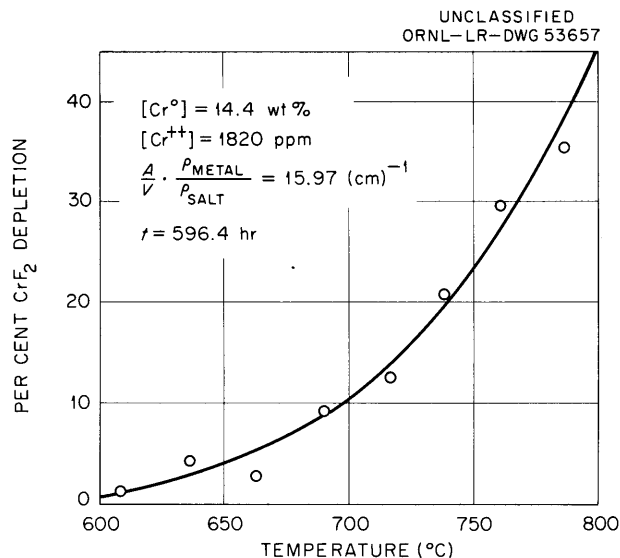
Fig. A.5. Results of Polythermal Experiments with Inconel Capsules.

Procedures for Constant-Potential Experiments

As mentioned previously, the results of experiments based on depletion methods revealed that the CrF_2 content of the salt will remain essentially constant if the alloy container is first equilibrated with respect to Eq. (1) for several hours at 900°C, then subjected to lower temperatures. A small specimen of the identical alloy subsequently immersed in the salt will pick up labeled chromium under conditions of a constant surface potential; that is, the Cr^0 concentration at the specimen surface, C_0, is constant with time.

A diagram of the constant-potential apparatus is shown in Fig. A.6. The alloy specimens were isothermally exposed to the salts in the form of a closed, 1/4-in.-OD thermocouple well. The container or "pot" resided in a standard 1-in. tube furnace which was controlled to within ±3°C of the desired temperature. Temperatures within the well were periodically measured with a standard Pt vs 90% Pt–10% Rh thermocouple and a K-2 potentiometer. Filtered salt samples for counting and CrF_2 analyses were obtained when the wells were changed. An argon sweep created a "blanket" for these manipulations and also created agitation during short-term experiments. The argon sweep was discontinued during long-term tests to minimize plugging by the slightly volatile ZrF_4. Temperature gradients

thus introduced were negligible. Periodic hydrogen reduction of the system between runs kept the concentrations of corrosive NiF_2 and FeF_2 near their lower limit of detection.

The results of typical experiments conducted under comparable conditions are shown graphically in Fig. A.7. The curves indicate that Eq. (12)

$$\Delta M_{Cr^{o*}} = 2AC_{Cr^{o*}} \sqrt{\frac{Dt}{\pi}}$$

$$\Delta M_{Cr^{o*}} = 2A\rho_{METAL} \frac{[Cr^{o}][Cr^{+++}]}{[Cr^{++}]} \sqrt{\frac{Dt}{\pi}}$$

$$\frac{1}{A} \cdot \frac{\Delta M_{Cr^{o*}}}{[Cr^{+++}]} = \left(2\rho_{METAL} \frac{[Cr^{o}]}{[Cr^{++}]} \sqrt{\frac{D}{\pi}}\right)\sqrt{t}$$
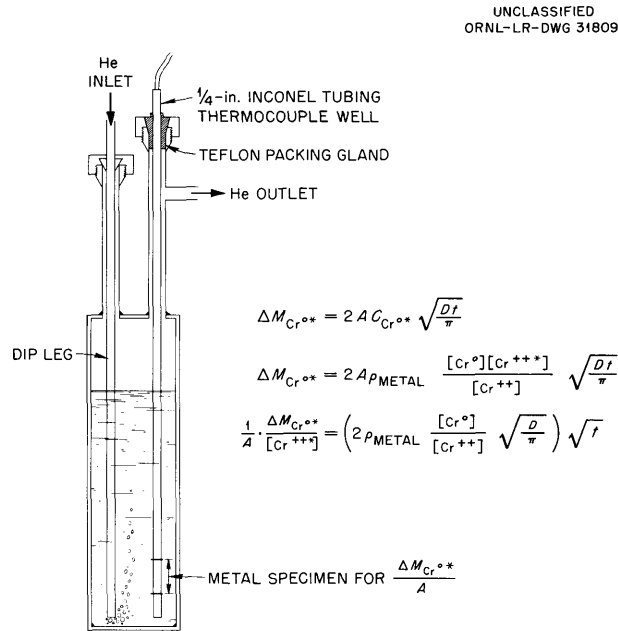
Fig. A.6. Apparatus and Equations for a Constant-Potential Diffusion Experiment.
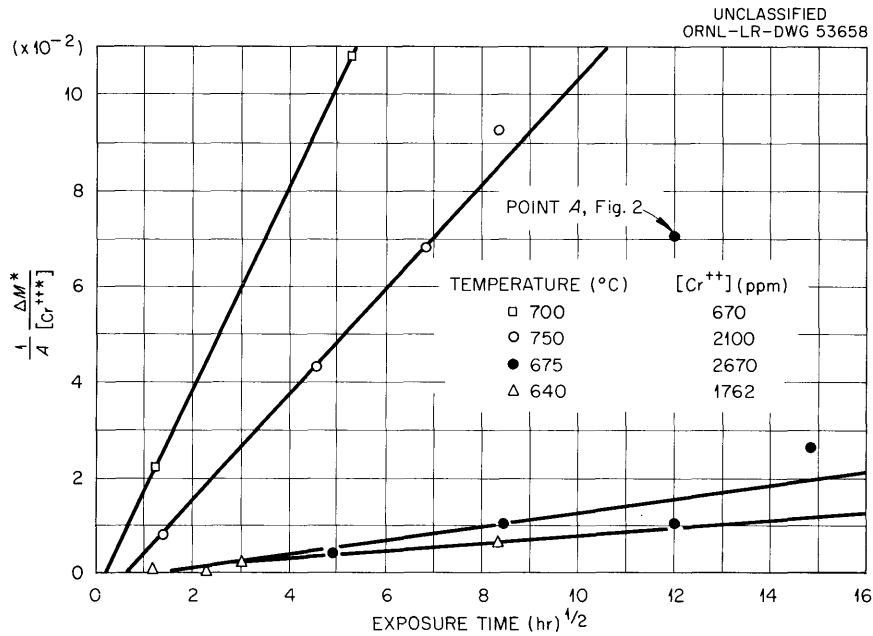
Fig. A.7. Time Dependence Curves for Constant-Potential Experiments.

is followed, although the intercept of many of the curves did not occur precisely at the origin. In these cases the slopes of the lines as shown were utilized to obtain the corresponding coefficients.

Pretreated wells were stored in evacuated tubes before and after salt exposure; caution was exercised during removal of the well from the salt to avoid surface oxidation. At a convenient time the exposed wells were cut up to furnish specimens for counting, electropolishing, and Cr^0 analyses. The generalized curve used to correlate the electropolishing data is shown as curve B in Fig. A.4.

INTERNAL DISTRIBUTION

1. R. D. Ackley
2. R. E. Adams
3. G. M. Adamson, Jr.
4. L. G. Alexander
5. J. W. Allen
6. C. F. Baes
7. C. J. Barton
8. P. R. Bell
9. M. Bender
10. R. L. Bennett
11. E. S. Bettis
12. D. S. Billington
13. J. P. Blakely
14. M. Blander
15. F. F. Blankenship
16. E. P. Blizard
17. C. M. Blood
18. A. L. Boch
19. E. G. Bohlmann
20. B. S. Borie
21. C. J. Borkowski
22. W. F. Boudreau
23. G. E. Boyd
24. M. A. Bredig
25. E. J. Breeding
26. R. B. Briggs
27. K. B. Brown
28. W. E. Browning
29. F. R. Bruce
30. J. H. Burns
31. S. Cantor
32. G. I. Cathers
33. C. E. Center
34. R. A. Charpie
35. T. E. Cole
36. E. L. Compere
37. J. A. Conlin
38. J. H. Coobs
39. W. B. Cottrell
40. J. A. Cox
41. J. H. Crawford, Jr.
42. F. L. Culler
43. H. N. Culver
44. D. R. Cuneo
45. J. E. Cunningham
46. J. H. DeVan
47. R. S. Cockreham
48. F. A. Doss
49. D. A. Douglas, Jr.
50. J. S. Drury
51. L. C. Emerson
52. L. B. Emlet (K-25)
53. J. E. Eorgan
54. E. P. Epler
55. R. B. Evans III
56. H. L. Falkenberry
57. D. E. Ferguson
58. J. Foster
59. J. L. Fowler
60. A. P. Fraas
61. E. U. Franck
62. H. A. Friedman
63. J. H. Frye, Jr.
64. C. H. Gabbard
65. G. A. Garrett (K-25)
66. J. S. Gill
67. J. H. Gillette
68. L. O. Gilpatrick
69. B. L. Greenstreet
70. J. M. Googin (Y-12)
71. W. R. Grimes
72. E. Guth
73. W. O. Harms
74. C. S. Harrill
75. G. M. Hebert
76. H. L. Hemphill
77. R. F. Hibbs (Y-12)
78. T. Hikido
79. M. R. Hill
80. E. E. Hoffman
81. H. W. Hoffman
82. A. Hollaender
83. A. S. Householder
84. H. Inouye
85. H. Insley
86. G. H. Jenks
87. E. V. Jones
88. W. H. Jordan
89. P. R. Kasten
90. G. W. Keilholtz

91.	C. P. Keim	143.	J. H. Shaffer
92.	M. J. Kelly	144.	R. P. Shields
93.	M. T. Kelley	145.	E. D. Shipley
94.	C. R. Kennedy	146.	M. D. Silverman
95.	J. J. Keyes	147.	O. Sisman
96.	B. W. Kinyon	148.	M. J. Skinner
97.	R. B. Korsmeyer	149.	R. Slusher
98.	J. A. Lane	150.	G. P. Smith, Jr.
99.	C. G. Lawson	151.	N. V. Smith
100.	J. E. Lee	152.	A. H. Snell
101.	S. A. Levin (K-25)	153.	B. A. Soldano
102.	T. A. Lincoln	154.	H. H. Stone
103.	S. C. Lind	155.	E. Storto
104.	R. B. Lindauer	156.	R. A. Strehlow
105.	R. S. Livingston	157.	R. D. Stulting
106.	T. S. Lundy	158.	B. J. Sturm
107.	R. N. Lyon	159.	C. D. Susano
108.	H. G. MacPherson	160.	J. A. Swartout
109.	W. D. Manly	161.	A. Taboada
110.	E. R. Mann	162.	E. H. Taylor
111.	W. L. Marshall	163.	R. E. Thoma
112.	H. C. McCurdy	164.	W. C. Thurber
113.	W. B. McDonald	165.	D. B. Trauger
114.	H. F. McDuffie	166.	J. Truitt
115.	C. J. McHargue	167.	E. Von Halle (K-25)
116.	F. R. McQuilkin	168.	C. S. Walker
117.	H. J. Metz	169.	J. L. Wantland
118.	A. J. Miller	170.	W. T. Ward
119.	C. E. Miller	171.	G. M. Watson
120.	R. E. Moore	172.	C. F. Weaver
121.	K. Z. Morgan	173.	A. M. Weinberg
122.	J. P. Murray (Y-12)	174.	J. C. White
123.	F. H. Neill	175.	E. A. Wick
124.	M. L. Nelson	176.	G. C. Williams
125.	R. F. Newton	177.	C. E. Winters
126.	L. G. Overholser	178.	L. B. Yeatts
127.	P. Patriarca	179.	J. Zasler
128.	F. S. Patton (Y-12)	180.	P. H. Emmett (consultant)
129.	A. M. Perry	181.	F. T. Gucker (consultant)
130.	D. Phillips	182.	F. Daniels (consultant)
131.	M. L. Picklesimer	183.	F. T. Miles (consultant)
132.	W. T. Rainey	184.	H. Eyring (consultant)
133.	J. D. Redman	185.	D. G. Hill (consultant)
134-135.	P. M. Reyling	186.	C. E. Larson (consultant)
136.	G. Samuels	187.	W. O. Milligan (consultant)
137.	A. R. Saunders	188.	J. E. Ricci (consultant)
138.	H. W. Savage	189.	G. T. Seaborg (consultant)
139.	A. W. Savolainen	190.	E. P. Wigner (consultant)
140.	J. L. Scott	191.	Biology Library
141.	H. E. Seagren	192.	Health Physics Library
142.	C. H. Secoy	193-194.	Central Research Library

195-214. Laboratory Records Department
  215. Laboratory Records, ORNL R.C.
  216. Reactor Division Library
  217. ORNL Y-12 Technical Library, Document Reference Section

EXTERNAL DISTRIBUTION

  218. L. Brewer, University of California
  219. Division of Research and Development, AEC, Washington
  220. Division of Research and Development, AEC, ORO
  221. Division of Reactor Development, AEC, Washington
  222. Division of Reactor Development, AEC, ORO
223-779. Given distribution as shown in TID-4500 (15th ed.) under
         Chemistry-General category (75 copies-OTS)